Taylor & Francis
Taylor & Francis Group

Check for updates

In silico identification and validation of natural antiviral compounds as potential inhibitors of SARS-CoV-2 methyltransferase

Anshuman Chandra[a]*, Meenakshi Chaudhary[b]*, Imteyaz Qamar[a], Nagendra Singh[a] (iD) and Vikrant Nain[a]

[a]School of Biotechnology, Gautam Buddha University, Greater Noida, India; [b]Department of Life Sciences, School of Natural Sciences, Shiv Nadar University, Greater Noida, India

Communicated by Ramaswamy H. Sarma

ABSTRACT

The novel Coronavirus disease 2019 (COVID-19) is potentially fatal and caused by Severe Acute Respiratory Syndrome Coronavirus 2 (SARS-CoV-2). Due to the unavailability of any proven treatment or vaccination, the outbreak of COVID-19 is wreaking havoc worldwide. Hence, there is an urgent need for therapeutics targeting SARS-CoV-2. Since, botanicals are an important resource for several efficacious antiviral agents, natural compounds gaining significant attention for COVID-19 treatment. In the present study, methyltranferase (MTase) of the SARS-CoV-2 is targeted using computational approach. The compounds were identified using molecular docking, virtual screening and molecular dynamics simulation studies. The binding mechanism of each compound was analyzed considering the stability and energetic parameter using *in silico* methods. We have found four natural antiviral compounds Amentoflavone, Baicalin, Daidzin and Luteoloside as strong inhibitors of methyltranferase of SARS-CoV-2. ADMET prediction and target analysis of the selected compounds showed favorable results. MD simulation was performed for four top-scored molecules to analyze the stability, binding mechanism and energy requirements. MD simulation studies indicated energetically favorable complex formation between MTase and the selected antiviral compounds. Furthermore, the structural effects on these substitutions were analyzed using the principles of each trajectories, which validated the interaction studies. Our analysis suggests that there is a very high probability that these compounds may have a good potential to inhibit Methyltransferase (MTase) of SARS-CoV-2 and to be used in the treatment of COVID-19. Further studies on these natural compounds may offer a quick therapeutic choice to treat COVID-19.

Abbreviations: ADMET: absorption, distribution, metabolism, excretion and toxicity; HIA: human intestinal absorption; MTase: methyltransferase; SAM: S-adenosyl methionine; SARS-CoV-2: Severe Acute Respiratory Syndrome Coronavirus 2; SBVS: structure-based virtual screening; tPSA: topological polar surface area

Introduction

COVID-19 is a highly infectious disease caused by Severe Acute Respiratory Syndrome Coronavirus 2 (SARS-CoV-2). The virus, originating in the city of Wuhan, China, was classified in the Coronavirus family (Boopathi et al., 2020; Caso & Federico, 2020; Lu et al., 2020; Wang et al., 2020). The pandemic caused by the virus is a great global public health concern. SARS-CoV-2 has a very high infection rate yet there is no reliable therapeutic interventions available to combat the illness (El Asnaoui & Chawki, 2020; Lu et al., 2020). The outbreak of COVID-19 has devastated humanity, crippled the economy and is retaining much of the human population in quarantine worldwide (Chan, Kok, et al., 2020; Vellingiri et al., 2020). Without an effective treatment, the threat of COVID-19, and consequent potential fatalities, will persist and may have detrimental effect globally (https://www.who.int/emergencies/diseases/novel-Coronavirus—2019).

Of the three beta Coronaviruses (MERS-CoV, SARS-CoV and SARS-CoV-2) that have infected the human population in the last decade, SARS-CoV-2 is the most infectious and lethal (S. Khan et al., 2020; Wang et al., 2020). The SARS-CoV-2 virus (also known as WH-Human-1 Coronavirus and 2019-nCoV) is classified in the Family *Coronaviridae* and is closely related to SARS-CoV (∼89%) (Mousavizadeh & Ghasemi, 2020).

The lack of availability of any approved treatment for COVID-19 necessitates an immediate need to find novel drugs for its cure. Scientific approaches to find COVID-19 treatments are in process like testing existing broad-spectrum antiviral drugs, such as cyclophilin, interferons and ribavirin. Another approach toward finding an effective treatment is drug repurposing that includes the screening of existing drug molecules

for anti-SARS-CoV-2 activity (R. J. Khan et al., 2020). Recent advances in robotics automated microfluidic system-based high-throughput screening makes drug repurposing a workable choice. Identification of drug targets from existing genomic information is also widely accepted to find therapeutics. Further, functional and structural characterization of the target enzymes is followed by identification of target inhibitors. Once identified, clinical trials are conducted on the lead compounds.

Many reports to find potential inhibitors using structure-based drug design studies have highlighted repurposing of FDA approved drugs (Adeoye et al., 2020). The potential targets for which the development of effective drugs against SARS-CoV-2 are in progress are summarized in Table S1. Molecular docking allows *in silico* screening of compounds before testing experimentally. This method has gained popularity in order to save time and resources in the drug discovery and development process (Gupta et al., 2018).

Coronavirus has a positive-sense, single-stranded RNA genome (Chan, Yuan, et al., 2020; Khailany et al., 2020; Mousavizadeh & Ghasemi, 2020). It has two overlapping open reading frames (ORF1a and ORF1b) that occupy two-thirds of the Coronavirus genome. These two ORFs are translated into polyproteins, pp1a and pp1ab, via a translational frameshift (Mousavizadeh & Ghasemi, 2020). These two polyproteins are processed to generate 16 non-structural proteins (nsp1 to 16) (Mousavizadeh & Ghasemi, 2020). The remaining portion of the genome includes ORFs for the structural proteins: spike (S), envelope (E), membrane (M) and nucleoprotein (N) and a variable number of accessory proteins (Mousavizadeh & Ghasemi, 2020).

One of the crucial proteins responsible for viral replication and expression in host cells is non-structural protein 16 (nsp16) or 2′-O-ribose methyltransferase (2′-OMTase or MTase) (Benkert et al., 2011; R. J. Khan et al., 2020). MTase modifies the viral genome by adding a 5′-terminal cap (m7GpppN) making it structurally similar to the host cell RNA. It allows the viral RNA to camouflage and escape the host cell defense mechanisms (Chen et al., 2011; R. J. Khan et al., 2020; Lugari et al., 2010). Since SARS-CoV-2 MTase is essential for the viral replication and is a good drug target candidate for COVID-19. The inhibition of MTase would enable the immune system to detect the virus and eliminate it from the cell.

Traditional medicines are one of the oldest treatments in human history, passed down for generations primarily by word of mouth (Vellingiri et al., 2020). Plant-based traditional compounds may in fact provide new inroads into global health care needs (Thangavel, 2021). These traditional plant-based remedies contain many constituents that either work alone, or in combination with other compounds, to produce the desired pharmacological effect.

The present study utilizes a systematic approach to find natural antiviral compounds extracted from plant species. These compounds might act as promising inhibitors against MTase of SARS-CoV-2. Through an extensive *in silico* approach, the aim of this study is to understand the underlying inhibitory mechanisms of these compounds. In order to accomplish this, molecular docking and molecular dynamics (MD) simulation studies have been used to calculate various

structural parameters including the estimated binding free energy (ΔG) of the drugs, Root Mean Square Deviation (RMSD), Root Mean Square Fluctuation (RMSF), Radius of Gyration (Rg), Solvent Accessible Surface Area (SASA), Principal Component Analysis (PCA) and the intermolecular hydrogen bonds (H-bonds) for free and inhibitor bounded SARS-CoV-2 MTase enzyme. Further *in vivo* and *in vitro* studies of these compounds will provide inroads for the development of novel anti-SARS-CoV-2 MTase inhibitors that emerge as good candidate drugs for COVID-19 therapy.

Material and methods

Preparation of ligands and receptor

The 3D SDF structure library of 348 antiviral compounds was downloaded from the SELLEKCHEM database (https://www.selleckchem.com). The compounds were imported into OpenBabel using the PyRx Tool (Dallakyan & Olson, 2015) and subjected to energy minimization. The energy minimization was performed with the universal force field (UFF) using the conjugate gradient algorithm. The total number of steps was set to 200 and the number of steps for the update was set to 1. In addition, the minimization was set to stop at an energy difference of less than 0.1 kcal/mol. The structures were converted to the PDBQT format for docking.

The structure of the SARS-CoV-2 MTase protein complex with SAM (S-Adenosyl methionine) (PDB-ID: 6W4H at resolution 1.80 Å) was used in the present study. The ligand SAM was removed from the structure for further docking studies. The receptor preparation was done using the protein preparation wizard tool of maestro Schrödinger (Sastry et al., 2013). Hydrogens were added and optimized by a hydrogen-bonding network in order to find the Histidine protonation state.

Docking

Blind docking was performed using the Autodock Vina tool compiled in the PyRx 0.8 virtual screening tool (Dallakyan & Olson, 2015; Trott & Olson, 2010). The search space encompassed the entire 3D structure chain A with the following dimensions in Å: center x, y, $z = 91.8653$, 24.0515, 23.3615, dimensions x, y, $z = 25$, 25, 25. The docking simulation was run at an exhaustiveness of 8 and set to output only the lowest energy poses. The top hit molecules, targeting specific residues of the SARS-CoV-2 MTase protein, were selected. Top four natural compounds (Amentoflavone, Baicalin, Daidzin and Luteoloside) with good binding affinity to SARS-CoV-2 MTase were selected for further analysis. Results were analyzed by LigPlot$^+$v.2.2 (Laskowski & Swindells, 2011).

In silico ADMET prediction

Pharmacokinetic parameters of absorption, distribution, metabolism, excretion and toxicity (ADMET) play a significant role in the discovery of novel drug candidates, as many invented drugs fail in the development process. Hence, the

in silico ADMET evaluation was computed using online SwissADME (https://www.swissadme.ch) (Daina et al., 2014, 2017; Daina & Zoete, 2016) and PreADMET (S. K. Lee et al., 2003, 2004) web tools.

Toxicology prediction of small molecules is important to predict the amount of tolerability of small molecules before being physiologically appropriated. The pkCSM online database (http://biosig.unimelb.edu.au/pkcsm/prediction) was used for toxicology prediction analysis (Pires et al., 2015). The website provides details of toxicology effects in the fields of AMES Toxicity, Human Maximum Tolerance Dose, hERG-I Inhibitor, hERG-II Inhibitor, LD50, LOAEL, Hepatotoxicity, Skin Toxicity, *T. pyriformis* toxicity and Minnow Toxicity.

Target prediction

Molecular Target studies are important to find the phenotypical side effects or potential cross reactivity caused by the action of small biomolecules (Gfeller et al., 2014; Keiser et al., 2007). Swiss Target Prediction website (http://www.swisstargetprediction.ch/) (Daina et al., 2019) was used for the target prediction analysis.

MD simulations

MD simulations of SARS-CoV-2 apo-MTase complexed with identified natural antiviral compounds were performed using the GROMACS software package using the GROMOS96 54a7 force field (Pronk et al., 2013; Van Der Spoel et al., 2005). The best pose of each MTase complex was used for MD simulation studies. The ligand topology was generated by the PRODRG server (Schuttelkopf & Van Aalten, 2004). Each complex was centered in a dodecahedron box with a minimum edge distance of 10 Å from the edge. The dodecahedron box was solvated with water molecules and 0.15 M NaCl. After system preparation, the system was energy minimized to avoid any steric hindrance by choosing the steepest descent method for a maximum of 5000 steps (Fmax < 100 kJ/mol/nm).

Further, to equilibrate the system at a constant temperature of 300 K in a two-step ensemble process, i.e. NVT and NPT were used for 100 ps. Finally, all systems were introduced to MD simulation. For analysis, conformations of MTase in each system were studied for the whole 100 ns trajectory. The trajectories were analyzed using g_gyrate, g_hbond, g_rmsf, g_rms and trajconv tools of GROMACS. All presentation was prepared using Chimera and Origin 6.0. (Chandra et al., 2021, 2020; Chetri et al., 2019; Kalita et al., 2019; Pandey, 2020; Shukla et al., 2019).

Results and discussion

Docking

To identify a potential SARS-CoV-2 MTase inhibitor, the structure-based molecular docking approach was performed on 348 antiviral compounds. These selected compounds have therapeutic potential against many infectious diseases, including anti-malarial and antiviral activities. All 348 compounds and S-Adenosyl methionine (SAM) (the SARS-CoV-2 MTase substrate) were docked with the SARS-CoV-2 chain A using blind docking. Out of these antiviral compounds, 160 compounds were found to have a binding energy between −9.3 and −6 kcal/mol (Table S2).

All of the compounds, including SAM, docked in the same cavity of the SARS-CoV-2 MTase (Figure 1 and Table S2). Primary screening showed that out of the 348 compounds, 18 had a docking score ranging from −9.3 to −8 kcal/mol (Figure S1 and Table S2). The list of the compounds, based on the binding energies (Vina scores) of the highest ranked position in the ligand docked with SARS-CoV-2 MTase, is shown in Table S2. The observed binding energy of SAM with the SARS-CoV-2 MTase complex was −7.3 kcal/mol (Table S2). A compound is predicted to have activity against a protein when it has a binding energy less than −6.0 kcal/mol (Shityakov & Förster, 2014).

Four natural antiviral compounds were analyzed for molecular interactions in the SARS-CoV-2 MTase complex (Table 1). The ligand interactions of SAM showed nine hydrogen bonds with five residues, Asp6928, Lys6968, Asn6996, Ser6999 and Glu7001. In addition, there were six hydrophobic interactions with residues Gly6869, Asp6897, Met6929, Tyr6930, Pro6932 and Thr6970 (Table S2).

Amentoflavone, having the lowest binding energy of −9.3 kcal/mol, has also been shown to bind to the SARS-COV-2 protease (Strodel et al., 2020). The results showed four hydrogen bonds with three MTase residues, Lys6844, Asn6996 and Ser6999. Amentoflavone also showed hydrophobic interactions with Asp6897, Leu6898, Asp6928, Met6929, Tyr6930, Pro6932, Lys6968, Asn6996, Thr6970 and Glu7001 residues of the SARS-CoV-2 MTase enzyme. The interactions with Asp6897, Asp6928, Met6929, Tyr6930, Pro6932, Lys6968, Thr6970, Ser6999, Asn6996 and Glu7001 are similar to SAM (Table 1, Table S2 and Figure 2). H-bond interactions in both SAM and Amentoflavone, with distance, is given in Table S2.

In terms of their binding energies, the other potent antiviral natural compounds were Baicalin, Daidzin and Luteoloside (Table 1, Table S2 and Figures 1 and 2).

Baicalin has also been recently targeted against the SARS-CoV-2 main protease (Islam et al., 2020) exhibiting a −8.7 kcal/mol binding energy with SARS-CoV-2 MTase. The interaction study showed seven hydrogen bonds with residues, Asn6841, Lys6844, Gly6871, Asp6897 and Asp6928. Baicalin showed several hydrophobic interactions with Gly6869, Ser6872, Leu6898, Tyr6930, Asp6931, Pro6932, Lys6968, Ser6999 and Glu7001 residues of the SARS-CoV-2 MTase, out of which the eight residues, Gly6869, Asp6897, Asp6928, Tyr6930, Pro6932, Lys6968, Ser6999 and Glu7001 were in common with the substrate SAM (Table 1, Table S2 and Figures 1 and 2).

Daidzin is also identified as strong binder of the SARS-CoV-2 spike protein in previous reports (Elfiky, 2020). Results showed a −8.3 kcal/mol binding energy with MTase. Daidzin bound MTase through six hydrogen bonds with residues Asp6897, Asn6899, Asp6928 and Tyr6930 along with several hydrophobic interactions with Lys6844, Gly6871, Ser6872, Met6929, Lys6968, Ser6999 and Glu7001 residues. The interactions with Asp6897, Asp6928, Met6929, Tyr6930, Lys6968,
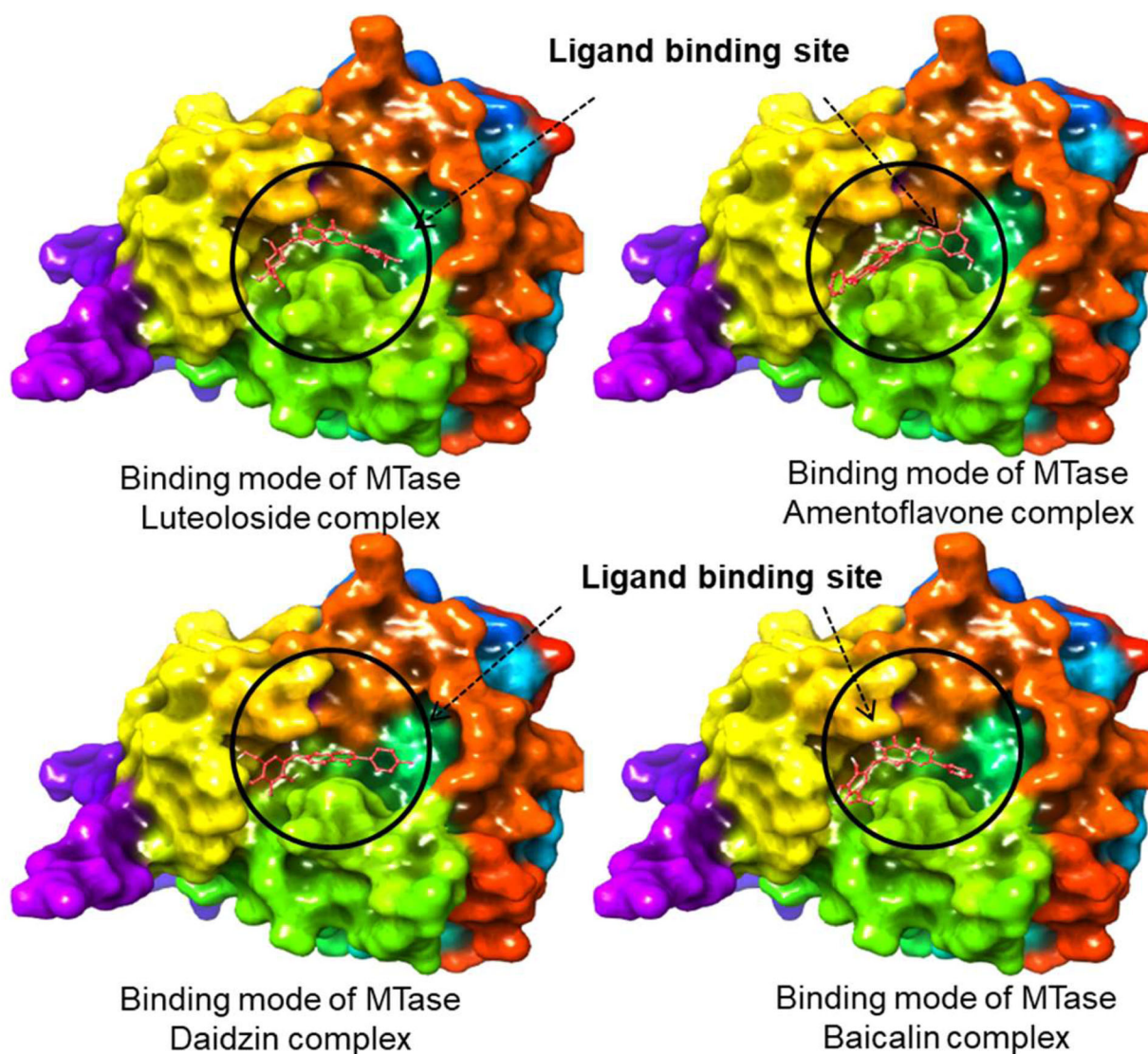
Figure 1. The surface rendition diagram. Binding mode of docked compounds in the active site of the SARS-CoV-2 MTase protein. The ligand is shown in the ball and stick conformation in red.

Ser6999 and Glu7001 were in common with the substrate SAM (Table 1, Table S2 and Figures 1 and 2).

Luteoloside has a −8.3 kcal/mol binding energy with MTAse. It binds the enzyme with eight hydrogen bonds on residues Asn6841, Lys6844, Gly6871, Asp6897, Asp6928, Tyr6930 and Ser6999. Luteoloside also formed several hydrophobic interactions with Gly6869, Asp6931, Lys6968, Thr6970 and Glu7001 residues of the SARS-CoV-2 MTase. Interactions with Gly6869, Asp6897, Tyr6930, Lys6968, Thr6970, Ser6999 and Glu7001 were common with the substrate SAM (Table 1, Table S2 and Figures 1 and 2). Other compounds also showed good binding affinities (Table S2).

In silico ADME prediction

ADME predictions of the four selected natural compounds were carried out. Parameters such as molecular weight (MW), hydrogen bond acceptor (HBA), hydrogen bond donor (HBD), number of rotatable bonds (n-rot-b), topological polar surface area (TPSA), partition coefficient (LogPo\w), aqueous

solubility (LogS), blood-brain barrier permeability (BBB), cytochrome-P2D6 inhibitor (CYP2D6), Lipinski rule of 5, hERG inhibition, human intestinal absorption (HIA) and PAINS alert were studied. The identified compounds were predicted to be non-toxic and showed lead likeliness.

The ADME predictions of all four natural compounds are summarized in Table S3 and Figures S2 and S3. Of the four natural compounds studied, two showed less than ten hydrogen bond acceptors (HBA) with the exception of Baicalin and Luteoloside (HBA-11). In addition, less than five hydrogen bond donors (HBD) were only found in Daidzin (HBD-5). The number of rotatable bonds in each molecule was less than 10.

The topological polar surface area (TPSA) was observed between 149.82 to 190.28 Å^2 (Table S3). The partition coefficient between n-octanol and water (LogPo/w) is the standard descriptor for hydrophobicity. All four natural compounds studied were found to have Log P values less than 5 (ranging between 0.20 and 3.62), showing good permeability across the cell membrane (Table S3). These parameters showed that the studied compounds obeyed Lipinski's rule

Table 1. Interaction and distance between the inhibitors and key amino acids of SARS-CoV-2 MTase in docking complexes determined using LIGPLOT program.

S. No	Compound name	Binding affinity (kcal/mol)	H-Bonds Residue (Atom Number-Distance in Å-Ligand atom number) Ligand	Other interactions (Total hydrophobic interacting residues)
1.	S-Adenosyl methionine	−7.3	S-Asn6996(ND-3.05-O4) L, S-Glu7001(OE1-3.00-O4) L, S-Lys6968(NZ-3.22-O3) L, S-Lys6968(NZ-3.06-O5) L, S-Asp6928(OD2-3.11-O5)L, S-Asp6928(OD-2.70-O2)L, B-Asp6928(O-2.98-O2)L, S-Ser6999(OG-3.17-O4)L, S-Ser6999(OG-2.34-N6)L	(6) Gly6869, Asp6897, Met6929, Tyr6930, Pro6932, Thr6970
2.	Amentoflavone	−9.3	S-Lys6844(NZ-2.97-O9)L, S-Lys6844(NZ-2.87-O7)L, S-Asn6996(ND-3.05-O4)L, S-Ser6999(OG-2.91-O10)L	(10) Asp6897, Leu6898, Asp6928, Met6929, Tyr6930, Pro6932, Lys6968, Asn6996, Thr6970, Glu7001
3.	Baicalin	−8.7	S-Asn6841(OD1-2.70-O11)L, S-Asn6841(ND2-3.15-O3)L, S-Lys6844(NZ-3.08-O2)L, B-Gly6871(O-2.72-O10)L, S-Asp6897(OD1-2.99-O4)L, S-Asp6897(OD1-2.93-O5)L, B-Asp6928(O-2.84-O11)L	(9) Gly6869, Ser6872, Leu6898, Tyr6930, Asp6931, Pro6932, Lys6968, Ser6999, Glu7001
4.	Daidzin	−8.3	S-Asp6897(OD1-2.96-O5)L, S-Asn6899(OD1-2.85-O6)L, B-Asp6928(O-3.10-O8)L, B-Tyr6930(O-3.20-O7)L, B-Tyr6930(O-3.02-O8)L, B-Tyr6930(N-2.87-O8)L	(7) Lys6844, Gly6871, Ser6872, Met6929, Lys6968, Ser6999, Glu7001
5.	Luteoloside	−8.3	S-Asn6841(ND2-3.14-O2)L, S-Asn6841(OD1-2.75-O9)L, S-Lys6844(NZ-3.20-O2)L, B-Gly6871(O-2.94-O8)L, S-Asp6897(OD1-2.76-O9)L, S-Asp6928(OD1-2.88-O9)L, B-Tyr6930(O-2.94-O5)L, S-Ser6999(OG-2.86-O10)L	(5) Gly6869, Asp6931, Lys6968, Thr6970, Glu7001

Abbreviations: S-Side chain, B-backbone, L-ligand.

of five (Lipinski et al., 2001) with only two violations, and, therefore, could be used as orally active antiviral agents.

Drug solubility is a significant property influencing absorption. Also, a water-soluble compound facilitates the ease of formulation and oral administration in order to deliver enough quantity of the active ingredient (Daina et al., 2017). All four compounds were found soluble. Human intestinal absorption (HIA) is the sum of the absorption and bioavailability that is estimated from the ratio of excretion or cumulative excretion in bile, urine and feces. Drugs are considered well absorbed if the intake lies between 70–100%. All the selected natural compounds showed an intestinal absorption between 25.16–88.20% (Amentoflavone-88.20%, Baicalin-32.42%, Daidzin-69.57% and Luteoloside-25.16%) as shown in Table S3.

Toxicity prediction

The results showed that none of the compounds cross the blood-brain barrier, thereby decreasing the possibility of neurotoxicity (Table S3 and Figure S2). In addition, the results showed that none of the compounds inhibited CYP2D6, a crucial isoenzyme belonging to the superfamily of cytochrome P450 (CYP450). CYP2D6 is responsible for metabolizing most of the drugs in the liver (Rydberg & Olsen, 2012). Inhibition of CYP2D6 causes drug-drug interactions leading to toxic effects (Daina et al., 2017). Thus, the

observation that none of the studied compounds inhibited CYP2D6 is a significant finding ruling out metabolic toxicity. In a related toxicity correlate, diabetic patients are at higher risk of developing cardiovascular disease (Aldossari, 2018). The inhibition of human hERG leads to fatal ventricular tachyarrhythmia via a prolonged QT interval (Guth & Rast, 2010). Of the four compounds, Amentoflavone and Daidzin were found to be at medium risk of hERG inhibition while Luteoloside was found to be at high risk and Baicalin was ambiguous (Tables S3 and S4 and Figure S3).

The pKCSM program-based *in silico* toxicity scores revealed that none of the four natural compounds showed AMES toxicity (Table S4). Likewise, none of the compounds showed inhibition of hERG-I. However, three compounds (Amentoflavone, Daidzin and Luteoloside) showed hERG-II inhibition potential (Table S4). For hepatotoxicity, Daidzin was predicted to have toxicity potential. All of the compounds showed maximum *T. pyriformis* toxicity range (0.285 to 0.287log μg/L). The lowest Fathead Minnow toxicity was observed for Amentoflavone at 0.801 mM (Table S4).

Target prediction

The *in silico* potential target prediction of four natural compounds in the human proteome are summarized in Table S5 and Figure S4. The targets of Amentoflavone were predicted to be the family AG protein-coupled receptors (20%), kinase
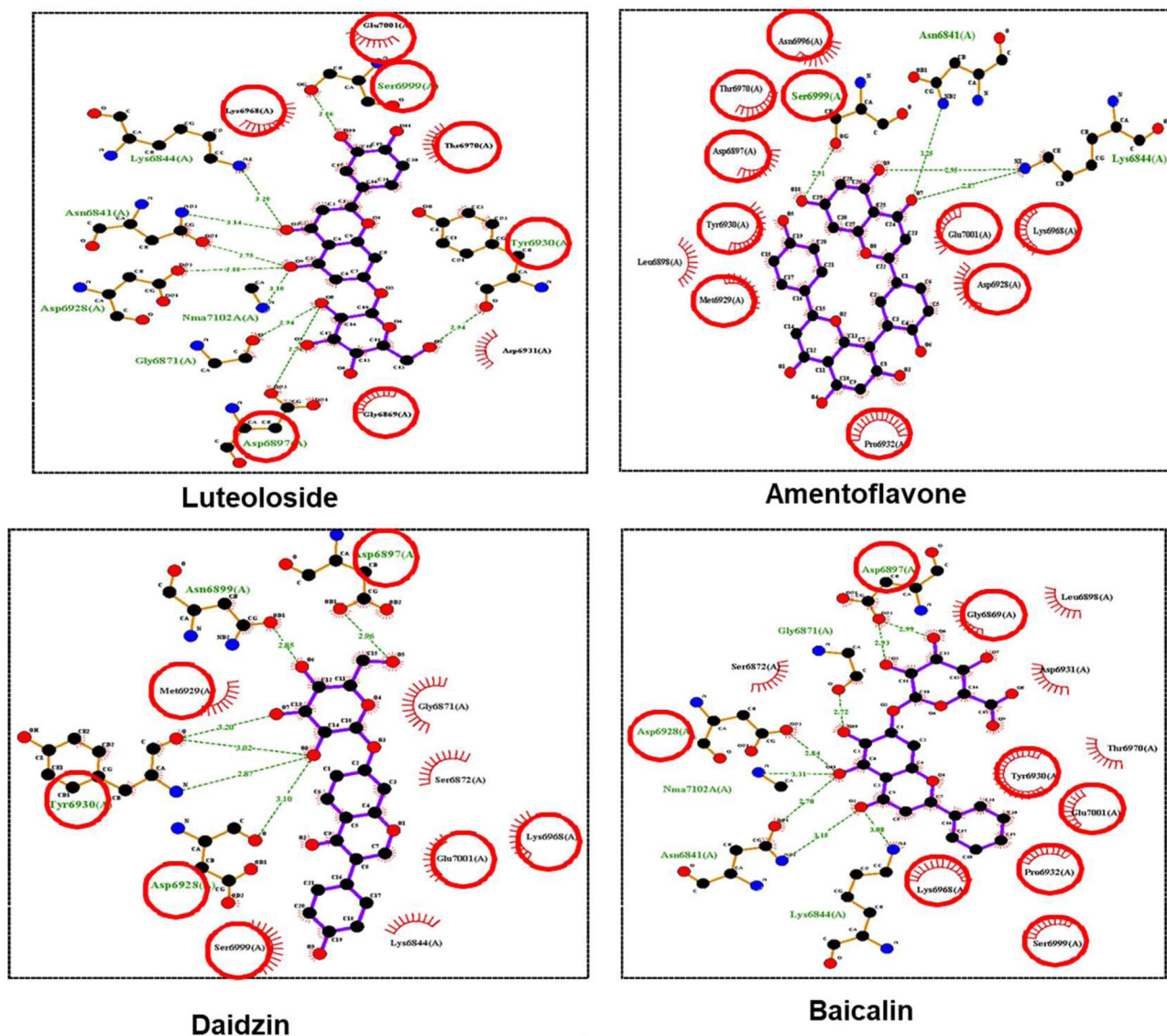
Figure 2. The 2D interaction diagram. The docked poses displaying interactions in the SAM binding site of the SARS-CoV-2 MTase protein. In the diagrams, residues highlighted in with a red circle are common with SAM binding residues in the SARS-CoV-2 MTase complexes.

(13.3%), enzymes (13.3%), unclassified proteins (13.3%), primary active transporters, secreted proteins, ligand-gated ion channels, phosphatases and proteases (6.7%) with a probability of 1%. This indicates that for Amentoflavone there is the probability of having off-target activity in humans (Figure S5 and Table S5).

Baicalin showed a potential target with enzymes (20%) but with a very low probability of 0.15%. In addition, Baicalin showed a potential target of family AG protein-coupled receptors (26.7%) but with a very low probability (0.12%) of having off-target activity in humans (Figure S5 and Table S5). In Daidzin, there was a potential target with oxidoreductases (13.3%) and secreted proteins (20%) with a probability of 1% each (Figure 5S and Table S5). Likewise, Luteoloside showed a potential target of secreted proteins (13.3%) with a probability of 0.81%, enzymes (20%) with a probability of 0.33%, oxidoreductases (13.3%) with the probability 0.16%, and family AG protein-coupled receptors (26.7%) with a probability of 0.15%. These data indicate that for Luteoloside there is a

very low probability of having off-target activity in humans (Figure S4 and Table S5).

The output table comprising Target, Common Name, Uniprot ID, ChEMBL-ID, Target Class, Probability and known actives in 2D/3D for Amentoflavone, Baicalin, Daidzin and Luteoloside is summarized in Table S5.

Molecular dynamics simulation

To infer MTase dynamics, MD simulation studies were carried out. Fundamental properties like deviation, fluctuation and compactness of the structure during a simulation provides insights into protein stability in thermodynamics. The RMSD for each system was computed considering 100 ns trajectories. For MTase, the RMSD calculation of the Cα backbone was selected. All of the systems showed minimal deviations and remained stable during the simulation period. The average RMSD for the apo-MTase, MTase-Amentoflavone, MTase-Baicalin, MTase-Diadizin and MTase-Luteoloside complexes was raised to be 0.35 nm, 0.266 nm, 0.25 nm, 0.32 nm and
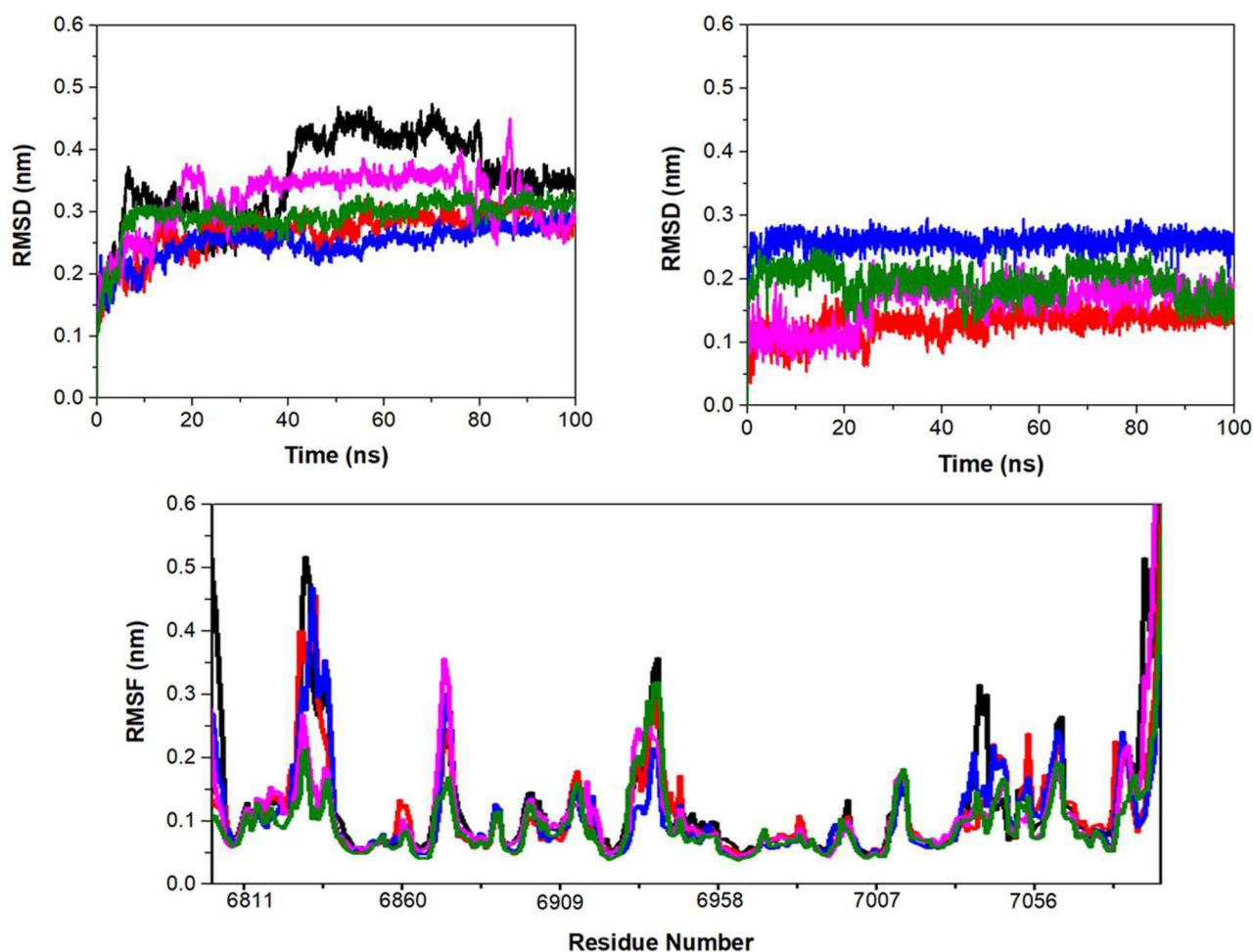
Figure 3. Molecular dynamics simulation of MTase from SARS-CoV-2. RMSD of the Cα backbone of apo-MTase and its complexes regarding time (100 ns), RMSD of drugs over 100 ns, RMSF of Cα atoms of the MTase complexes over 100 ns. The apo-MTase (black) complexed with Amentoflavone (red), Baicalin (blue), Diadizin (Magenta) and Luteoloside (green) are represented.

0.29 nm, respectively. All Inhibitor-MTase systems attained equilibrium at 50 ns since the apo-MTase was stabilized after 80 ns. The MTase-Diadizin complex showed a peak of 86 ns at 0.4 nm. The RMSD of each Inhibitor-MTase complex was less than the apo-MTase, suggesting a stable conformation of MTase upon binding to inhibitors (Figure 3). The RMSD of each ligand was also calculated to elucidate changes in the binding pattern. The average RMSD of Amentoflavone, Baicalin, Diadizin and Luteoloside was 0.127 nm, 0.25 nm, 0.16 nm and 0.193 nm, respectively (Figure 3). All of the systems attained equilibrium after 50 ns of simulation. Further analysis of stability parameters for each complex was carried out for the last 50 ns.

In order to understand the residue-wise fluctuations between the apo-MTase and Inhibitor-MTase complexes, the RMSF values were plotted. The average RMSF values for apo-MTase, MTase-Amentoflavone, MTase-Baicalin, MTase-Diadizin and MTase- Luteoloside complex were found to be 0.136 nm, 0.115 nm, 0.11 nm, 0.117 nm and 0.09 nm, respectively. In apo-MTase, the loop region Gly6829 to Met6839 and Leu7037 to Ser7041 showed significant fluctuations of 50 Å and 30 Å, respectively. No significant fluctuations were observed with Inhibitor-MTase complexes. All of the Inhibitor-MTase complexes showed a comparable RMSF (Figure 3). The RMSF of the MTase-Luteoloside complex was

least among all of the complexes, suggesting a stable binding. Also, protein compactness is a significant factor in determining the folded state. The Rg was calculated to measure the compactness of MTase in all systems. It was observed that all systems had comparable Rg values with no significant changes in the simulation. The average Rg for the apo-MTase, MTase-Amentoflavone, MTase-Baicalin, MTase-Diadizin and MTase-Luteoloside complex was found to be 1.86 nm, 1.85 nm, 1.84 nm, 1.85 nm and 1.83 nm, respectively (Figure 4). Compactness analysis suggested that identified compounds formed attractive and stable interactions with MTase.

Intermolecular polar interaction between protein and ligand plays a crucial role in the binding affinity. The hydrogen bond between MTase and each of the compounds was calculated for the last 50 ns of simulation. The maximum number of hydrogen bonds in MTase-Amentoflavone, MTase-Baicalin, MTase-Diadizin and MTase-Luteoloside complex was found to be 8, 7, 7 and 9, respectively (Figure 4). Luteoloside formed the highest number of hydrogen bonds among all of the drugs. The results showed that in the presence of the identified drug, the binding pocket of MTase remains stable, suggesting that the identified drugs molecules have a high affinity toward MTase and can be used as potential binders of MTase. The SASA was then calculated to decipher protein
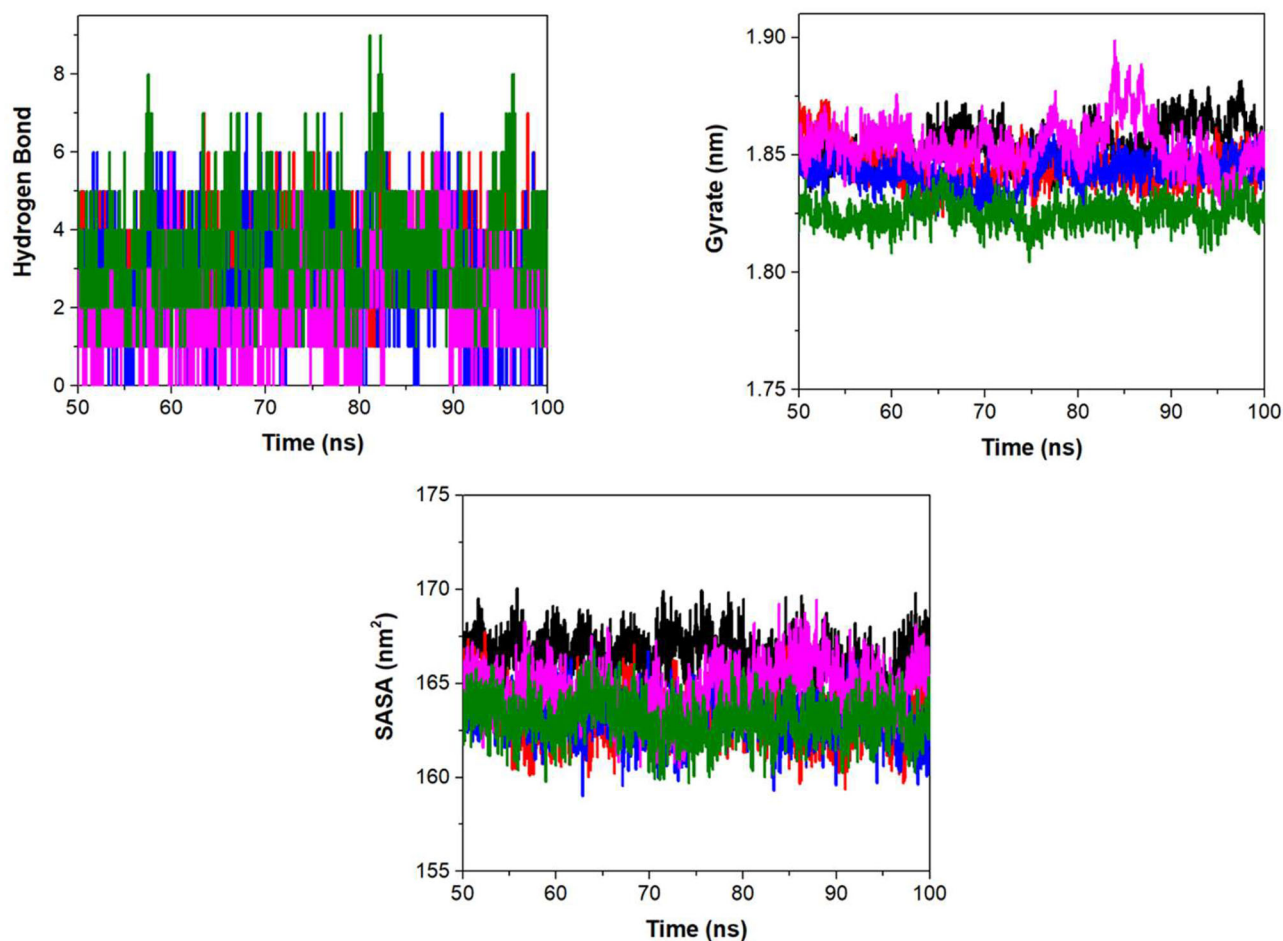
Figure 4. Stability of MTase from SARS-CoV-2. The number of hydrogen bond interactions between MTase and drugs during the simulation is shown. The radius of gyration (Rg) of MTase alone and in the complex with drugs over the course of the simulation. The total solvent-accessible area with respect to time is shown. The apo-MTase (black) complexed with Amentoflavone (red), Baicalin (blue), Diadizin (Magenta) and Luteoloside (green) are represented.
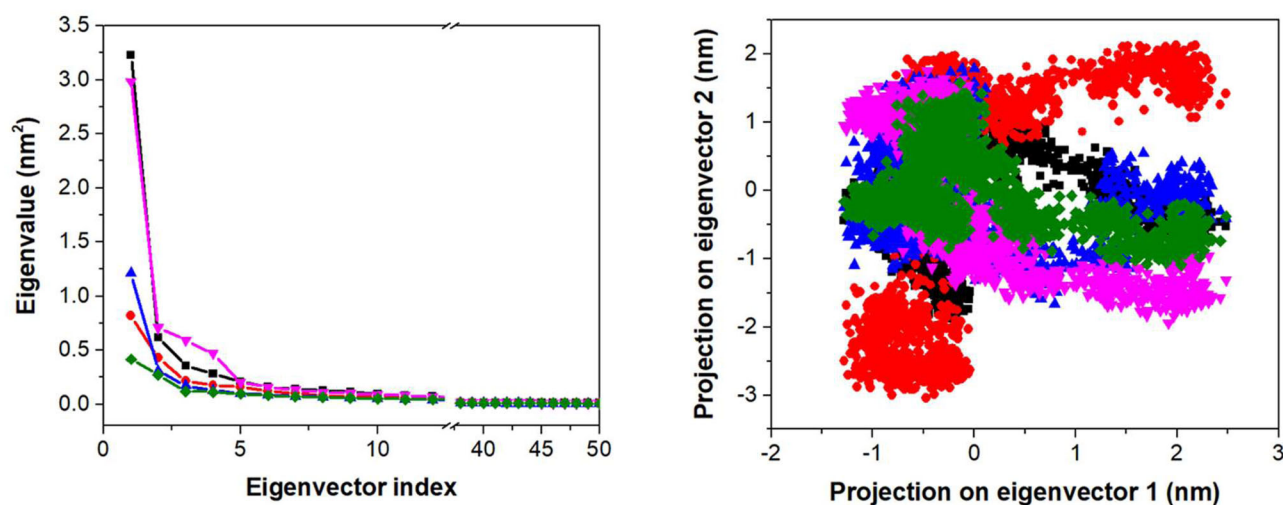

Figure 5. PCA of MTase from SARS-CoV-2 Plot of eigenvalues against the eigenvector index is shown. Only the top 50 eigenvectors were considered for representation. Projections of the motion of the MTase in the first two principal component vectors (PC1 vs PC2). The apo-MTase (black) complexed with Amentoflavone (red), Baicalin (blue), Diadizin (Magenta) and Luteoloside (green) are represented.

stability and folding during the simulation (Figure 4). The SASA plot showed lower SASA values for MTase-Amentoflavone, MTase-Baicalin and MTase-Luteoloside while for MTase-Diadizin, it showed higher SASA values. The average value for the apo-MTase, MTase-Amentoflavone, MTase-

Baicalin, MTase-Diadizin and MTase- Luteoloside complex was found to be 166 nm^2, 163 nm^2, 164 nm^2, 165 nm^2 and 163 nm^2, respectively. From these results, it can be concluded that Amentoflavone, Baicalin, Diadizin and Luteoloside showed good binding to MTase.

Principal component analysis

PCA is a method to simplify complex data with minimum information loss. In this study, the correlated motions were predicted by using PCA. The eigenvalues were derived for all of the complexes and the first ten hits were considered for analysis. The data showed motions of 82%, 72%, 75%, 84% and 65% for apo-MTase, MTase-Amentoflavone, MTase-Baicalin, MTase-Diadizin and MTase-Luteoloside, respectively (Figure 5). The figure shows that apo-MTase exhibited the highest motions of all the drug-MTase complexes. Imputing drug-MTase, the drugs showed fewer motions. From the overall analysis, it is predicted that the drugs Amentoflavone, Baicalin, Diadizin and Luteoloside are less motion inducing thereby providing stability to the drug-MTase complex. Then, the first two eigenvectors were selected and plotted against each other (PC1 vs PC2). In this plot, that apo-MTase showed multiple clusters compared to the identified drugs (Figure 5). The MTase-Luteoloside complex showed dense and stable clusters. The cluster of MTase-Amentoflavone, MTase-Baicalin and MTase-Diadizin was also stable compared to apo-MTase.

Conclusions

Viral respiratory infections are prevalent, and they can be eliminated from the body with no detrimental consequences (Hendaus & Jomha, 2020). Recently, natural compounds have received attention as novel antiviral therapeutics. Thus, identifying natural ingredients to advance antiviral treatments holds good possibilities for new treatments. Amentoflavonea, a well-known biflavonoid found in many natural plants, has been shown to exhibit anti-oxidation (Saroni Arwa et al., 2015), anti-tumor (Chiang et al., 2019), anti-inflammatory (Funakoshi-Tago et al., 2015), neuro-protective (Zhang et al., 2015) and cardiovascular protective properties (Gan et al., 2021; Zheng et al., 2013). Baicalin (5, 6-dihydroxy-7-O-glucuronide flavone) is a drug used for adjuvant therapy of hepatitis in traditional Chinese medicine (Tao et al., 2018). Baicalin is a dominant flavonoid and has various pharmacological activities, including anti-oxidative (Y.-C. Lee et al., 2008), antiviral (Huang et al., 2000), anti-inflammatory (Huang et al., 2006), anti-HIV (Li et al., 1993) and anti-proliferative properties (Tao et al., 2018). Daidzin is a natural organic compound in the class of phytochemicals known as isoflavones (Rafii, 2015), and is found in leguminous plants, especially soybeans (Keung et al., 1997). It is a potent and selective inhibitor of human mitochondrial aldehyde dehydrogenase (ALDH-2) (Keung et al., 1997). Luteoloside (luteolin-7-O-glucoside) is found in some types of dried fruits and a variety of other plant sources such as *Lonicera japonica*, 'Jinyinhua' in Chinese, is an important herbal plant that has been widely used in Chinese medicine for thousands of years. This naturally occurring flavonoid is also isolated from the medicinal plant *Gentiana macrophylla*. Luteoloside exhibits several bio-activities, including anti-microbial and anti-cancer activities, and was also shown to act as a 3 C protease inhibitor of EV-A71 *in vitro* (Cao et al., 2016). No serious adverse events have been reported for these selected compounds. However, there have been few studies about safety in pregnant women and people with underlying medical conditions. Drug-likeness factor rules were obeyed accordingly with no violation by these four compounds. Thus, these natural compounds can act as a drug in biological systems. The toxicity prediction says that they are safe and can be given as drugs with the value of tolerance prescribed for human consumption. All of the four natural compounds (Amentoflavone, Baicalin, Daidzin and Luteoloside) showed favorable ADMET properties. Molecular dynamics simulation studies showed stable conformation dynamics upon compound binding to MTase. Hence, all four compounds, Amentoflavone, Baicalin, Daidzin and Luteoloside, can be considered for their exceptional binding energy and ADMET properties. However, further investigation and validation of these inhibitors against SARS-CoV-2 are needed to claim their candidacy for clinical trials.

Disclosure statement

Authors have no conflict of interest.

ORCID

Nagendra Singh http://orcid.org/0000-0003-0419-0684

References

Adeoye, A. O., Oso, B. J., Olaoye, I. F., Tijjani, H., & Adebayo, A. I. (2020). Repurposing of chloroquine and some clinically approved antiviral drugs as effective therapeutics to prevent cellular entry and replication of coronavirus. *Journal of Biomolecular Structure and Dynamics*. Advance online publication. https://doi.org/10.1080/07391102.2020.1765876

Aldossari, K. K. (2018). Cardiovascular outcomes and safety with antidiabetic drugs. *International Journal of Health Sciences*, *12*(5), 70–83.

Benkert, P., Biasini, M., & Schwede, T. (2011). Toward the estimation of the absolute quality of individual protein structure models. *Bioinformatics (Oxford, England)*, *27*(3), 343–350. https://doi.org/10.1093/bioinformatics/btq662

Boopathi, S., Poma, A. B., & Kolandaivel, P. (2020). Novel 2019 coronavirus structure, mechanism of action, antiviral drug promises and rule out against its treatment. *Journal of Biomolecular Structure and Dynamics*. Advance online publication. https://doi.org/10.1080/07391102.2020.1758788

Cao, Z., Ding, Y., Ke, Z., Cao, L., Li, N., Ding, G., Wang, Z., & Xiao, W. (2016). Luteoloside acts as 3C protease inhibitor of enterovirus 71 in vitro. *PLoS One*, *11*(2), e0148693. https://doi.org/10.1371/journal.pone.0148693

Caso, V., & Federico, A. (2020). No lockdown for neurological diseases during COVID19 pandemic infection. *Neurological Sciences: Official Journal of the Italian Neurological Society and of the Italian Society of Clinical Neurophysiology*, *41*(5), 999–1001. https://doi.org/10.1007/s10072-020-04389-3

Chandra, A., Ananda, H., Singh, N., & Qamar, I. (2021). Identification of a novel and potent small molecule inhibitor of SRPK1: Mechanism of dual inhibition of SRPK1 for the inhibition of cancer progression. *Aging (Albany NY)*, *13*, 163–180. https://doi.org/10.18632/aging.202301

Chandra, A., Goyal, N., Qamar, I., & Singh, N. (2020). Identification of hot spot residues on serine-arginine protein kinase-1 by molecular dynamics simulation studies. *Journal of Biomolecular Structure and Dynamics*. Advance online publication. https://doi.org/10.1080/07391102.2020.1734487

Chan, J. F.-W., Kok, K.-H., Zhu, Z., Chu, H., To, K. K.-W., Yuan, S., & Yuen, K.-Y. (2020). Genomic characterization of the 2019 novel human-pathogenic coronavirus isolated from a patient with atypical pneumonia after visiting Wuhan. *Emerging Microbes & Infections*, *9*(1), 221–236. https://doi.org/10.1080/22221751.2020.1719902

Chan, J. F.-W., Yuan, S., Kok, K.-H., To, K. K.-W., Chu, H., Yang, J., Xing, F., Liu, J., Yip, C. C.-Y., Poon, R. W.-S., Tsoi, H.-W., Lo, S. K.-F., Chan, K.-H., Poon, V. K.-M., Chan, W.-M., Ip, J. D., Cai, J.-P., Cheng, V. C.-C., Chen, H., Hui, C. K.-M., & Yuen, K.-Y. (2020). A familial cluster of pneumonia associated with the 2019 novel coronavirus indicating person-to-person transmission: A study of a family cluster. *The Lancet*, *395*(10223), 514–523. https://doi.org/10.1016/S0140-6736(20)30154-9

Chen, Y., Su, C., Ke, M., Jin, X., Xu, L., Zhang, Z., Wu, A., Sun, Y., Yang, Z., Tien, P., Ahola, T., Liang, Y., Liu, X., & Guo, D. (2011). Biochemical and structural insights into the mechanisms of SARS coronavirus RNA ribose 2′-O-methylation by nsp16/nsp10 protein complex. *PLoS Pathogens*, *7*(10), e1002294. https://doi.org/10.1371/journal.ppat.1002294

Chetri, P. B., Shukla, R., & Tripathi, T. (2019). Identification and characterization of glyceraldehyde 3-phosphate dehydrogenase from *Fasciola gigantica*. *Parasitology Research*, *118*(3), 861–872. https://doi.org/10.1007/s00436-019-06225-w

Chiang, C.-H., Yeh, C.-Y., Chung, J. G., Chiang, I.-T., & Hsu, F.-T. (2019). Amentoflavone induces apoptosis and reduces expression of anti-apoptotic and metastasis-associated proteins in bladder cancer. *Anticancer Research*, *39*(7), 3641–3649. https://doi.org/10.21873/anticanres.13512

Daina, A., Michielin, O., & Zoete, V. (2014). iLOGP: A simple, robust, and efficient description of n-octanol/water partition coefficient for drug design using the GB/SA approach. *Journal of Chemical Information and Modeling*, *54*(12), 3284–3301. https://doi.org/10.1021/ci500467k

Daina, A., Michielin, O., & Zoete, V. (2017). SwissADME: A free web tool to evaluate pharmacokinetics, drug-likeness and medicinal chemistry friendliness of small molecules. *Scientific Reports*, *7*, 42717. https://doi.org/10.1038/srep42717

Daina, A., Michielin, O., & Zoete, V. (2019). SwissTargetPrediction: Updated data and new features for efficient prediction of protein targets of small molecules. *Nucleic Acids Research*, *47*(W1), W357–W364. https://doi.org/10.1093/nar/gkz382

Daina, A., & Zoete, V. (2016). A BOILED-egg to predict gastrointestinal absorption and brain penetration of small molecules. *ChemMedChem*, *11*(11), 1117–1121. https://doi.org/10.1002/cmdc.201600182

Dallakyan, S., & Olson, A. J. (2015). Small-molecule library screening by docking with PyRx. *Methods in Molecular Biology (Clifton, N.J.)*, *1263*, 243–250. https://doi.org/10.1007/978-1-4939-2269-7_19

El Asnaoui, K., & Chawki, Y. (2020). Using X-ray images and deep learning for automated detection of coronavirus disease. *Journal of Biomolecular Structure and Dynamics*. Advance online publication. https://doi.org/10.1080/07391102.2020.1767212

Elfiky, A. A. (2020). SARS-CoV-2 RNA dependent RNA polymerase (RdRp) targeting: an in silico perspective. *Journal of Biomolecular Structure & Dynamics*. Advance online publication. https://doi.org/10.1080/07391102.2020.1761882

Funakoshi-Tago, M., Okamoto, K., Izumi, R., Tago, K., Yanagisawa, K., Narukawa, Y., Kiuchi, F., Kasahara, T., & Tamura, H. (2015). Anti-inflammatory activity of flavonoids in Nepalese propolis is attributed to inhibition of the IL-33 signaling pathway. *International Immunopharmacology*, *25*(1), 189–198. https://doi.org/10.1016/j.intimp.2015.01.012

Gan, L., Ma, J., You, G., Mai, J., Wang, Z., Yang, R., Xie, C., Fei, J., Tang, L., Zhao, J., Cai, Z., & Ye, L. (2021). Glucuronidation and its effect on the bioactivity of amentoflavone, a biflavonoid from Ginkgo biloba leaves. *Journal of Pharmacy and Pharmacology*, *73*(1), 1–11. https://doi.org/10.1111/jphp.13247

Gfeller, D., Grosdidier, A., Wirth, M., Daina, A., Michielin, O., & Zoete, V. (2014). SwissTargetPrediction: A web server for target prediction of bioactive small molecules. *Nucleic Acids Research*, *42*(Web Server issue), W32–W38. https://doi.org/10.1093/nar/gku293

Gupta, M., Sharma, R., & Kumar, A. (2018). Docking techniques in pharmacology: How much promising? *Computational Biology and Chemistry*, *76*, 210–217. https://doi.org/10.1016/j.compbiolchem.2018.06.005

Guth, B. D., & Rast, G. (2010). Dealing with hERG liabilities early: Diverse approaches to an important goal in drug development. *British Journal of Pharmacology*, *159*(1), 22–24. https://doi.org/10.1111/j.1476-5381.2009.00265.x

Hendaus, M. A., & Jomha, F. A. (2020). Covid-19 induced superimposed bacterial infection. *Journal of Biomolecular Structure and Dynamics*. Advance online publication. https://doi.org/10.1080/07391102.2020.1772110

Huang, R.-L., Chen, C.-C., Huang, H.-L., Chang, C.-G., Chen, C.-F., Chang, C., & Hsieh, M.-T. (2000). Anti-hepatitis B virus effects of wogonin isolated from *Scutellaria baicalensis*. *Planta Medica*, *66*(8), 694–698. https://doi.org/10.1055/s-2000-9775

Huang, W.-H., Lee, A.-R., & Yang, C.-H. (2006). Antioxidative and anti-inflammatory activities of polyhydroxyflavonoids of *Scutellaria baicalensis* GEORGI. *Bioscience, Biotechnology, and Biochemistry*, *70*(10), 2371–2380. https://doi.org/10.1271/bbb.50698

Islam, R., Parves, M. R., Paul, A. S., Uddin, N., Rahman, M. S., Mamun, A. A., Hossain, M. N., Ali, M. A., & Halim, M. A. (2020). A molecular modeling approach to identify effective antiviral phytochemicals against the main protease of SARS-CoV-2. *Journal of Biomolecular Structure & Dynamics*. Advance online publication. https://doi.org/10.1080/07391102.2020.1761883

Kalita, J., Shukla, R., & Tripathi, T. (2019). Structural basis of urea-induced unfolding of *Fasciola gigantica* glutathione S-transferase. *Journal of Cellular Physiology*, *234*(4), 4491–4503. https://doi.org/10.1002/jcp.27253

Keiser, M. J., Roth, B. L., Armbruster, B. N., Ernsberger, P., Irwin, J. J., & Shoichet, B. K. (2007). Relating protein pharmacology by ligand chemistry. *Nature Biotechnology*, *25*(2), 197–206. https://doi.org/10.1038/nbt1284

Keung, W. M., Klyosov, A. A., & Vallee, B. L. (1997). Daidzin inhibits mitochondrial aldehyde dehydrogenase and suppresses ethanol intake of Syrian golden hamsters. *Proceedings of the National Academy of Sciences of the United States of America*, *94*(5), 1675–1679. https://doi.org/10.1073/pnas.94.5.1675

Khailany, R. A., Safdar, M., & Ozaslan, M. (2020). Genomic characterization of a novel SARS-CoV-2. *Gene Reports*, *19*, 100682. https://doi.org/10.1016/j.genrep.2020.100682

Khan, R. J., Jha, R. K., Amera, G. M., Jain, M., Singh, E., Pathak, A., Singh, R. P., Muthukumaran, J., & Singh, A. K. (2020). Targeting SARS-CoV-2: A systematic drug repurposing approach to identify promising inhibitors against 3C-like proteinase and 2′-O-ribose methyltransferase. *Journal of Biomolecular Structure & Dynamics*. Advance online publication. https://doi.org/10.1080/07391102.2020.1753577

Khan, S., Siddique, R., Shereen, M. A., Ali, A., Liu, J., Bai, Q., Bashir, N., & Xue, M. (2020). Emergence of a novel coronavirus, severe acute respiratory syndrome coronavirus 2: Biology and therapeutic options. *Journal of Clinical Microbiology*, *58*(5), e00187–20. https://doi.org/10.1128/JCM.00187-20

Laskowski, R. A., & Swindells, M. B. (2011). LigPlot+: Multiple ligand-protein interaction diagrams for drug discovery. *Journal of Chemical Information and Modeling*, *51*(10), 2778–2786. https://doi.org/10.1021/ci200227u

Lee, S. K., Chang, G. S., Lee, I. H., Chung, J. E., Sung, K. Y., & No, K. T. (2004). The PreADME: Pc-based program for batch prediction of ADME properties. *EuroQSAR*, 9, 5–10.

Lee, Y.-C., Chuah, A. M., Yamaguchi, T., Takamura, H., & Matoba, T. (2008). Antioxidant activity of traditional Chinese medicinal herbs. *Food Science and Technology Research*, 14(2), 205–210. https://doi.org/10.3136/fstr.14.205

Lee, S. K., Lee, I. H., Kim, H. J., Chang, G. S., Chung, J. E., & No, K. T. (2003). The PreADME Approach: Web-based program for rapid prediction of physico-chemical, drug absorption and drug-like properties. In *EuroQSAR 2002 Designing Drugs and Crop Protectants: Processes, Problems and Solutions* (pp. 418–420). Blackwell Publishing.

Li, B. Q., Fu, T., Yan, Y. D., Baylor, N. W., Ruscetti, F. W., & Kung, H. F. (1993). Inhibition of HIV infection by baicalin–a flavonoid compound purified from Chinese herbal medicine. *Cellular & Molecular Biology Research*, 39(2), 119–124.

Lipinski, C. A., Lombardo, F., Dominy, B. W., & Feeney, P. J. (2001). Experimental and computational approaches to estimate solubility and permeability in drug discovery and development settings. *Advanced Drug Delivery Reviews*, 46(1-3), 3–26. https://doi.org/10.1016/S0169-409X(00)00129-0

Lu, H., Stratton, C. W., & Tang, Y. (2020). Outbreak of pneumonia of unknown etiology in Wuhan China: The mystery and the miracle. *Journal of Medical Virology*, 92(4), 401–402. https://doi.org/10.1002/jmv.25678

Lugari, A., Betzi, S., Decroly, E., Bonnaud, E., Hermant, A., Guillemot, J.-C., Debarnot, C., Borg, J.-P., Bouvet, M., Canard, B., Morelli, X., & Lécine, P. (2010). Molecular mapping of the RNA Cap 2′-O-methyltransferase activation interface between severe acute respiratory syndrome coronavirus nsp10 and nsp16. *Journal of Biological Chemistry*, 285(43), 33230–33241. https://doi.org/10.1074/jbc.M110.120014

Mousavizadeh, L., & Ghasemi, S. (2020). Genotype and phenotype of COVID-19: Their roles in pathogenesis. *Journal of Microbiology, Immunology and Infection*. Advance online publication. https://doi.org/10.1016/j.jmii.2020.03.022

Pandey, A. (2020). Reappraisal of trifluperidol against NSP-3 protein: Potential therapeutic for COVID-19. *Research Square*, 30. Advance online publication. https://doi.org/10.21203/rs.3.rs-52706/v1

Pires, D. E. V., Blundell, T. L., & Ascher, D. B. (2015). pkCSM: Predicting small-molecule pharmacokinetic and toxicity properties using graph-based signatures. *The Journal of Medicinal Chemistry*, 58(9), 4066–4072. https://doi.org/10.1021/acs.jmedchem.5b00104

Pronk, S., Páll, S., Schulz, R., Larsson, P., Bjelkmar, P., Apostolov, R., Shirts, M. R., Smith, J. C., Kasson, P. M., Van Der Spoel, D., Hess, B., & Lindahl, E. (2013). GROMACS 4.5: A high-throughput and highly parallel open source molecular simulation toolkit. *Bioinformatics (Oxford, England)*, 29(7), 845–854. https://doi.org/10.1093/bioinformatics/btt055

Rafii, F. (2015). The role of colonic bacteria in the metabolism of the natural isoflavone daidzin to equol. *Metabolites*, 5(1), 56–73. https://doi.org/10.3390/metabo5010056

Rydberg, P., & Olsen, L. (2012). Predicting drug metabolism by cytochrome P450 2C9: Comparison with the 2D6 and 3A4 isoforms. *ChemMedChem*, 7(7), 1202–1209. https://doi.org/10.1002/cmdc.201200160

Saroni Arwa, P., Zeraik, M. L., Ximenes, V. F., da Fonseca, L. M., Bolzani, V., da, S., & Siqueira Silva, D. H. (2015). Redox-active biflavonoids from *Garcinia brasiliensis* as inhibitors of neutrophil oxidative burst and human erythrocyte membrane damage. *Journal of Ethnopharmacology*, 174, 410–418. https://doi.org/10.1016/j.jep.2015.08.041

Sastry, G. M., Adzhigirey, M., Day, T., Annabhimoju, R., & Sherman, W. (2013). Protein and ligand preparation: Parameters, protocols, and influence on virtual screening enrichments. *Journal of Computer-Aided Molecular Design*, 27(3), 221–234. https://doi.org/10.1007/s10822-013-9644-8

Shityakov, S., & Förster, C. (2014). In silico predictive model to determine vector-mediated transport properties for the blood–brain barrier choline transporter. *Advances and Applications in Bioinformatics and Chemistry*, 7, 23–36. https://doi.org/10.2147/AABC.S63749.

Schuttelkopf, A. W., & Van Aalten, D. M. F. (2004). PRODRG: A tool for high-throughput crystallography of protein-ligand complexes. *Acta Crystallographica Section D: Biological Crystallography*, D60, 1355–1363. https://doi.org/10.1107/S0907444904011679

Shukla, R., Shukla, H., & Tripathi, T. (2019). Structural and energetic understanding of novel natural inhibitors of Mycobacterium tuberculosis malate synthase. *Journal of Cellular Biochemistry*, 120(2), 2469–2482. https://doi.org/10.1002/jcb.27538

Strodel, B., Olubiyi, O., Olagunju, M., Keutmann, M., & Loschwitz, J. (2020). High throughput virtual screening to discover inhibitors of the main protease of the coronavirus SARS-CoV-2. *Preprints*, 2020040161. https://doi.org/10.20944/preprints202004.0161.v1

Tao, Y., Zhan, S., Wang, Y., Zhou, G., Liang, H., Chen, X., & Shen, H. (2018). Baicalin, the major component of traditional Chinese medicine *Scutellaria baicalensis* induces colon cancer cell apoptosis through inhibition of oncomiRNAs. *Scientific Reports*, 8(1), 14477. https://doi.org/10.1038/s41598-018-32734-2

Thangavel, N. (2021). Molecular docking and molecular dynamics aided virtual search of OliveNet directory for secoiridoids to combat SARS-CoV-2 infection and associated hyperinflammatory responses. *Frontiers in Molecular Biosciences*, 7(January), 627767. https://doi.org/10.3389/fmolb.2020.627767

Trott, O., & Olson, A. J. (2010). AutoDock Vina: Improving the speed and accuracy of docking with a new scoring function, efficient optimization, and multithreading. *Journal of Computational Chemistry*, 31(2), 455–461. https://doi.org/10.1002/jcc.21334

Van Der Spoel, D., Lindahl, E., Hess, B., Groenhof, G., Mark, A. E., & Berendsen, H. J. C. (2005). GROMACS: Fast, flexible, and free. *Journal of Computational Chemistry*, 26(16), 1701–1718. https://doi.org/10.1002/jcc.20291

Vellingiri, B., Jayaramayya, K., Iyer, M., Narayanasamy, A., Govindasamy, V., Giridharan, B., Ganesan, S., Venugopal, A., Venkatesan, D., Ganesan, H., Rajagopalan, K., Rahman, P. K. S. M., Cho, S.-G., Kumar, N. S., & Subramaniam, M. D. (2020). COVID-19: A promising cure for the global panic. *Science of the Total Environment*, 725, 138277. https://doi.org/10.1016/j.scitotenv.2020.138277

Wang, C., Horby, P. W., Hayden, F. G., & Gao, G. F. (2020). A novel coronavirus outbreak of global health concern. *The Lancet*, 395(10223), 470–473. https://doi.org/10.1016/S0140-6736(20)30185-9

Zhang, Z., Sun, T., Niu, J.-G., He, Z.-Q., Liu, Y., & Wang, F. (2015). Amentoflavone protects hippocampal neurons: Anti-inflammatory, antioxidative, and antiapoptotic effects. *Neural Regeneration Research*, 10(7), 1125–1133. https://doi.org/10.4103/1673-5374.160109

Zheng, X., Liu, C., Zhai, Y., Li, L., Wang, X., & Feng, W. (2013). Protection effect of amentoflavone in *Selaginella tamariscina* against TNF-alpha-induced vascular injury of endothelial cells. *Yao Xue Xue Bao = Acta Pharmaceutica Sinica*, 48(9), 1503–1509.